

Gaussian variational ansatz in the problem of anomalous sea waves: Comparison with direct numerical simulations

V. P. Ruban*

Landau Institute for Theoretical Physics RAS, Moscow, Russia

(Dated: April 1, 2024)

The nonlinear dynamics of an obliquely oriented wave packet at sea surface is studied both analytically and numerically for various initial parameters of the packet, in connection with the problem of oceanic rogue waves. In the framework of Gaussian variational ansatz applied to the corresponding (1+2D) hyperbolic nonlinear Schrödinger equation, a simplified Lagrangian system of differential equations is derived, which determines the evolution of coefficients of the real and imaginary quadratic forms appearing in the Gaussian. This model provides a semi-quantitative description for the process of nonlinear spatio-temporal focusing, which is one of the most probable mechanisms of rogue wave formation in random wave fields. The system is integrated in quadratures, which fact allows us to understand qualitative differences between the linear and nonlinear regimes of the focusing of wave packet. Comparison of the Gaussian model predictions with results of direct numerical simulation of fully nonlinear long-crested water waves is carried out.

Key words: oceanic rogue waves, nonlinear focusing, variational approximation.

PACS numbers: 47.35.Bb, 47.10.Df, 02.30.Mv, 92.10.Hm

I. INTRODUCTION

Anomalous waves at the ocean surface and in many other physical systems (known also as giant waves, rogue waves, freak waves) have been a popular subject of present-day scientific research (see, e.g., reviews [1–3], and references therein). The most frequently used mathematical model for this phenomenon is the (1+1D) nonlinear Schrödinger equation (NLSE) with the focusing nonlinearity. In particular, such equation describes the complex amplitude of the main harmonic of a quasi-monochromatic weakly nonlinear surface wave over plane potential flows of an ideal fluid [4]. Due to nonlinear self-focusing, the modulation instability develops in a sufficiently lengthy and high wave group [4, 5]. As the result, a one-dimensional anomalous wave arises. Such a scenario is confirmed by numerical and laboratory experiments [6–11]. The full integrability makes the (1+1D) NLSE attractive for analytical studies and provides many exact solutions which describe some important properties of real rogue waves (see, e.g., [12–16]).

In the Nature however sea waves are rather far from the one-dimensional model (see, e.g., [17–23]). When on the free fluid surface there are disturbances depending on both horizontal coordinates, the wave dynamics becomes more complicated already in the framework of the corresponding NLSE, not to speak about strongly nonlinear regimes. First, (1+2D) NLSE is not integrable. Second, in the case of deep-water gravity waves, the spatial differential operator in it appears hyperbolic:

$$2i\psi_t + \psi_{xx} - \psi_{yy} + |\psi|^2\psi = 0. \quad (1)$$

Here the non-dimensional variables are in use: $k_0 A^* \rightarrow \psi$, $\omega_0 t \rightarrow t$, $2k_0 x \rightarrow x$, $\sqrt{2}k_0 y \rightarrow y$, where $A(x, y, t)$ is the complex envelope of the main harmonic, k_0 is the wave number, $\omega_0 = 2\pi/T_0 = \sqrt{gk_0}$ is the frequency of the carrier wave (the reference frame is moving with the group velocity $v_{gr} = (1/2)\sqrt{g/k_0}$ along x axis). Although Eq.(1) has some disadvantages, which are not discussed here, but it is more suitable for approximate analytical studies (because in all its modified variants, some pseudo-differential operators appear inevitably, difficult to calculate them “by hands”).

Thus, in the transverse direction the nonlinearity acts in the defocusing manner, while in the longitudinal direction it works for focusing of a wave packet. In addition, the linear dispersion makes its own defocusing contribution. Owing to the indicated factors, the behavior of a nonlinear group of waves on the two-dimensional free surface of the fluid is more diverse as compared to the one-dimensional case. Depending on initial conditions, the nonlinearity can in some cases reinforce the linear focusing, but as well it can destroy the focusing in other cases. In the case of reinforcement, a rogue wave arises. Besides that, anomalous waves can appear as a result of interaction between previously formed coherent structures [20]. However, for the usual oceanic wave fields where the presence of coherent structures is hardly probable, more actual seems the scenario when anomalous waves rise due to occasional spatio-temporal focusing (see [24, 25], and references therein).

In general, the question about optimal conditions for the nonlinear focusing of water waves is still far from being clear. It is only obvious that, similarly to the 1D case, the initial wave group should be sufficiently high and/or extensive. But an effect of geometric shape of the packet, as well as phase modulation, on the development of anomalous wave is poorly studied. In the absence

*Electronic address: ruban@itp.ac.ru

of exact (1+2D) NLSE solutions, which could describe quantitatively all such processes, it seems reasonable to carry out approximate consideration of the dynamics of an idealized solitary wave packet characterized by a few time-dependent parameters. Thereby, the above qualitative reasons could be concretized, and a reference point could be put along the direction of development of future more accurate theory of three-dimensional rogue waves.

The purpose of this work is to investigate the nonlinear dynamics of a wave packet in the framework of the full Gaussian variational ansatz, i.e. in the case when the quadratic form under the exponential has an off-diagonal part. Such a packet has an elliptical shape, with main axes oriented at some time-dependent angle with respect to the coordinate axes. Contrary to the more widely known diagonal ansatz (see, e.g., [26–34]), the full Gaussian ansatz was previously applied to the elliptic NLSE only [35, 36]. The present work fills this gap in the theory. Here a system of variational equations will be derived for parameters of the ellipse, and its full integrability will be demonstrated. The fact of integrability takes place, first, because the third power of the NLSE nonlinearity is accorded with the two spatial dimensions, and second, because Eq.(1) has a special integral of motion, namely the hyperbolic analog of the angular momentum,

$$\int i[y(\psi_x\psi^* - \psi\psi_x^*) + x(\psi_y\psi^* - \psi\psi_y^*)]dxdy = \text{const.} \quad (2)$$

The knowledge of general structure of analytical solutions of the variational model will allow us to understand qualitative differences between the linear and nonlinear regimes of the wave packet focusing. Besides that, with the purpose of immediate testing of the Gaussian model, a comparison between its predictions and the results of numerical simulations of fully nonlinear long-crested waves will be carried out. We shall see that the agreement can be rather good even for strongly nonlinear regimes, when the very NLSE is not applicable already.

II. VARIATIONAL ANSATZ

Let us first remind that in the simplest — diagonal — variant, the Gaussian ansatz describes an elliptical wave packet having the symmetry axes coinciding with the coordinate axes (see, e.g., [26–31]):

$$\psi = \sqrt{\frac{4N}{XY}} \exp \left[-\frac{x^2}{2X^2} - \frac{y^2}{2Y^2} + i\frac{Ux^2}{2X} - i\frac{Vy^2}{2Y} + i\phi \right]. \quad (3)$$

Besides the longitudinal size $X(t)$ and transverse size $Y(t)$, such a packet is characterized by four more real quantities: U , V , N , and ϕ . Parameter N does not depend on time because $4\pi N = \int |\psi|^2 dxdy$ is an exact integral of motion of NLSE, while the conjugate variable ϕ is cyclic. Parameters U and V describe a phase modulation, with positive/negative values of U or V corresponding to defocusing/focusing configurations respectively in x or y

direction. Here it is necessary to note that for applicability of NLSE, the condition of narrow spectral width of the wave packet should be satisfied. In our case it practically means the following: $(X, Y) \gtrsim 10$, $(U, V) \lesssim 0.1$. Equations of motion determining the temporal behavior of the unknown quantities X , Y , U , and V , are derived by substitution of the variational ansatz (3) into the Lagrangian functional of the NLSE:

$$\mathcal{L} = \int (i\psi_t\psi^* - i\psi\psi_t^* - |\psi_x|^2 + |\psi_y|^2 + |\psi|^4/2) dxdy. \quad (4)$$

In this way we obtain a reduced Lagrangian $\tilde{\mathcal{L}}$ depending on N , $X(t)$, $Y(t)$, $U(t)$, and $V(t)$. The action integral $\int \tilde{\mathcal{L}} dt$ should be then varied. The main outcome of this standard procedure is the following. Variation of the reduced action gives in particular that $U = \dot{X}$, $V = \dot{Y}$. Finally we arrive at the following system of differential equations of the Newtonian type:

$$\ddot{X} = \frac{1}{X^3} - \frac{N}{X^2Y}, \quad \ddot{Y} = \frac{1}{Y^3} + \frac{N}{Y^2X}. \quad (5)$$

Note that equations (5) constitute a Lagrangian system with the Lagrangian functional $L \propto \tilde{\mathcal{L}}/N$, where

$$2L = \dot{X}^2 - \dot{Y}^2 - \frac{1}{X^2} + \frac{1}{Y^2} + \frac{2N}{XY}, \quad (6)$$

so the kinetic energy is not positively-definite (the second “particle” has a negative mass).

It should be said that equations of the type (5) and their generalizations are actively used in plasma physics, in nonlinear optics, and in atomic physics to investigate behavior of NLSE and Gross-Pitaevskii equation solutions in two and three spatial dimensions (see papers [26–34], and references therein). In particular in work [27], analytical and some numerical solutions were presented namely for the hyperbolic (1+2D) NLSE, as in our case, but with such parameter values that are typical for nonlinear optics, not for water waves. In relation to the problem of anomalous sea wave focusing, this simplified variational ansatz was applied only very recently in the author’s work [37].

Let us now turn our attention to the full Gaussian ansatz, i.e. when off-diagonal elements of the quadratic forms are involved. For further consideration, it is convenient to introduce linear combinations of the spatial coordinates, corresponding to a hyperbolic rotation with the parameter χ (analogously to the elliptic NLSE case, but with the difference that there the rotation was usual trigonometric):

$$\bar{x} = x \cosh \chi + y \sinh \chi, \quad \bar{y} = x \sinh \chi + y \cosh \chi. \quad (7)$$

Instead of expression (3) we now write

$$\psi = \sqrt{\frac{4N}{XY}} \exp \left[-\frac{\bar{x}^2}{2X^2} - \frac{\bar{y}^2}{2Y^2} + i\frac{U\bar{x}^2}{2X} - i\frac{V\bar{y}^2}{2Y} - i\gamma\bar{x}\bar{y} + i\phi \right]. \quad (8)$$

Strictly speaking, with $\chi \neq 0$ the parameters X and Y are no longer the longitudinal and transverse sizes of the packet, but we shall continue to call them so for brevity. Parameter χ cannot be too large, otherwise the wave packet becomes spectrally wide and goes beyond the NLSE applicability domain. Practically, as it will be seen from the results of direct numerical simulation of nonlinear waves with realistic parameters, the inequality $|\chi| \lesssim 0.5$ should take place.

Note that Gaussian form (8) is one of exact solutions of the corresponding *linear* Schrödinger equation, with appropriate temporal dependencies of the parameters appearing there. Consequently, at small N the approximation (8) is certainly valid. In practice, values $N \approx 2-4$ are of interest. In this case, generally speaking, only qualitative agreement of the results of variational model (8) with the solutions of the NLSE (and, the more so, with the completely nonlinear dynamics of waves on water) can be expected. In more detail the comparison between the variational and numerical solutions will be discussed some later. An undoubted benefit of this approximation is that it provides a semiquantitative description of the process of spatio-temporal focusing, which is one of the most probable mechanisms of the formation of rogue waves under real conditions (see [24, 25], and references therein).

Having substituted the trial function (8) and its partial derivatives (expressed it terms of \bar{x} and \bar{y}) into the Lagrangian (4), after straightforward calculations we obtain that variable χ is cyclic, while the corresponding conserved quantity is (taking into account that $N = \text{const}$)

$$M = \gamma(X^2 + Y^2) = \text{const}. \quad (9)$$

Herewith, the temporal dependence of parameter χ is determined by the equation

$$\dot{\chi} = M(Y^2 - X^2)/(X^2 + Y^2)^2. \quad (10)$$

The conserved quantity M is a hyperbolic analog of the angular momentum. As previously, we have $U = \dot{X}$, $V = \dot{Y}$, but the dynamics of unknown functions $X(t)$ and $Y(t)$ is described now by the following Lagrangian:

$$2L_M = \dot{X}^2 - \dot{Y}^2 - \frac{1}{X^2} + \frac{1}{Y^2} + \frac{2N}{XY} + \frac{M^2(X^2 - Y^2)}{(X^2 + Y^2)^2}. \quad (11)$$

This Lagrangian is a hyperbolic analog of the elliptic variational problem considered in works [35, 36]. Equations of motion that follow from here, have the form

$$\ddot{X} = \frac{1}{X^3} - \frac{N}{X^2Y} + \frac{M^2X}{(X^2 + Y^2)^2} \left[1 - 2\frac{(X^2 - Y^2)}{(X^2 + Y^2)} \right], \quad (12)$$

$$\ddot{Y} = \frac{1}{Y^3} + \frac{N}{Y^2X} + \frac{M^2Y}{(X^2 + Y^2)^2} \left[1 - 2\frac{(Y^2 - X^2)}{(X^2 + Y^2)} \right]. \quad (13)$$

The finding solutions of this system and the comparison of the corresponding evolution of wave packet with a direct numerical modeling of nonlinear waves is the essence of the present work.

III. INTEGRABILITY OF THE MODEL

An important advantage of system (11) is an exact integrability, because here in analogy with the elliptic case, the separation of variables turns out to be possible. Integrability of the variational approximation is typical namely for NLSE in 2D space, because in 3D the reduced Lagrangian instead of $2N/(XY)$ would contain $2\tilde{N}/(XYZ)$, and it would destroy the homogeneity of the equations. It is well known from the analytical mechanics that for integration of the above system one should use the hyperbolic coordinates:

$$X = Q \sinh \xi, \quad Y = Q \cosh \xi. \quad (14)$$

These coordinates describe sector $X < Y$ which is most interesting in application to the problem of oceanic rogue waves, because a length of their crest usually 3–10 times exceeds the wave length $\lambda_0 = 2\pi/k_0$, while the longitudinal packet size in the minimum reaches approximately one λ_0 (that corresponds to dimensionless values $X_{\min} \sim 6-10$). The Lagrangian (11) takes the form

$$2L_M = Q^2\dot{\xi}^2 - \dot{Q}^2 - \frac{F(\xi)}{Q^2}, \quad (15)$$

where function $F(\xi)$ is defined by the formula

$$F(\xi) = \frac{4}{\sinh^2(2\xi)} - \frac{4N}{\sinh(2\xi)} + \frac{M^2}{\cosh^2(2\xi)}. \quad (16)$$

The corresponding equations of motion are

$$\ddot{Q} + Q\dot{\xi}^2 + \frac{F(\xi)}{Q^3} = 0, \quad (17)$$

$$2Q\dot{Q}\dot{\xi} + Q^2\ddot{\xi} + \frac{F'(\xi)}{2Q^2} = 0. \quad (18)$$

After multiplying Eq.(18) by $2Q^2\dot{\xi}$, we obtain in its left hand side a total time-derivative, so the integral of motion follows:

$$Q^4\dot{\xi}^2 + F(\xi) = C = \text{const}. \quad (19)$$

Looking at the expression (16), it is easy to understand that at sufficiently small negative values of the integration constant C , equation $F(\xi) = C$ determining “turn points”, has two real positive roots (ξ_1 and ξ_2), with the motion of variable ξ taking place between them. At $C \geq 0$ the “turn point” is sole.

Eq.(17) is simplified to $\ddot{Q} = -C/Q^3$. Its general solution is written in explicit form as

$$Q(t) = \sqrt{I(t - t_*)^2 - C/I}, \quad (20)$$

where t_* and I are two more integration constants. It is easy to check that $I = -2E$, where E is the energy integral of the system:

$$E = (Q^2\dot{\xi}^2 - \dot{Q}^2 + F(\xi)/Q^2)/2. \quad (21)$$

With taking into account Eq.(20), it follows from Eq.(19) that

$$\int_0^t \frac{dt}{I(t-t_*)^2 - C/I} = \pm \int_{\xi_0}^{\xi} \frac{d\xi}{\sqrt{C - F(\xi)}}, \quad (22)$$

where ξ_0 is the fourth — the last — integration constant. Formulas (20) and (22) provide the full solution of the problem. In particular, with $I > 0$, $C < 0$, the dependence (22) can be represented in the following form,

$$\sinh 2\xi(t) = P\left(a_0 + \frac{1}{\sqrt{-C}} \arctan\left[\frac{I(t-t_*)}{\sqrt{-C}}\right]\right), \quad (23)$$

where an even a -periodic function $P(a)$ (having a minimum at $a = 0$) is the inverse with respect to elliptic integral (here the integration variable $z = \sinh 2\xi$):

$$P\left(\pm \int_{s_1}^s \frac{zdz}{2\sqrt{(1+z^2)(Cz^2 + 4Nz - 4) - M^2z^2}}\right) \equiv s, \quad (24)$$

and s_1 is the smaller root of the equation $(1+s^2)(Cs^2 + 4Ns - 4) - M^2s^2 = 0$. The amplitude of wave packet equals to $\sqrt{4N/XY}$, and it is given by the formula

$$A(t) = \sqrt{8N}/\sqrt{[I(t-t_*)^2 - C/I] \sinh 2\xi(t)}. \quad (25)$$

IV. SELECTION OF THE SOLUTIONS

In fact, we shall not use the analytical solutions, expressed in terms of special functions, for finding the dependencies $X(t)$ and $Y(t)$ with some given initial values. Practically it is much simpler and faster to carry out highly accurate numerical simulation of the variational equations (12) and (13) immediately. One should also remember that the absolute accuracy in solving approximate variational problem is hardly necessary. The knowledge of the analytical structure of the solutions will be needed for a general understanding of properties of the dynamical system under consideration.

We are interested mainly in those solutions from the whole diversity (20) and (22), which result in essentially higher wave amplitude as compared to the maximally possible linear value $A_{\max \text{ lin}} = \sqrt{4NU_{-\infty}V_{-\infty}}$, where $U_{-\infty}$ and $V_{-\infty}$ are the asymptotic values of the focusing parameters at large negative times. In essence, only such events are deserving the terrible title “rogue waves”. What is important, the most interesting solutions correspond to values of the parameters $C \approx 0$, $M \approx 0$. The condition $C = 0$ means that $Q^2 \equiv Y^2 - X^2 = I(t-t_*)^2$, i. e. the plots of functions $X(t)$ and $Y(t)$ touch each other at $t = t_*$. It is easy to make sure of the above assertion by numerical simulations of Eqs.(12)-(13) [with fixed N , U_0 , V_0 , Y_0 , but different X_0 and M], and subsequent comparison of the maximal amplitudes. Typical dependencies $X(t)$ and $Y(t)$ for such a case are shown in Fig.1. Let us also note that the minimal value of the ratio $(X/Y)_{\min} = \tanh \xi_1$, which is reached closely to the

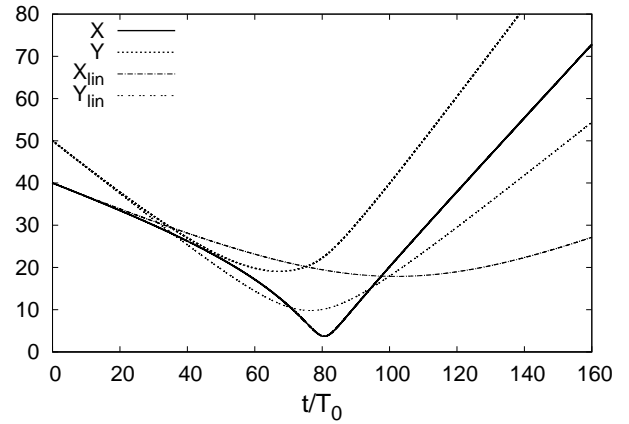


FIG. 1: The temporal dependencies $X(t)$ and $Y(t)$ for $N = 3.0$, $M = 0$, $X_0 = 40$, $Y_0 = 50$, $U_0 = -0.05$, $V_0 = -0.10$. The solutions for a linear packet with the same initial conditions are also shown for comparison. What is important for formation of a rogue wave, the nonlinear focusing along the longitudinal direction goes here with acceleration for most of the time, while in the linear case it occurs with deceleration for all the time. The value of X in the minimum has been too small for validity of the NLSE, but they are initial conditions of this type which in reality result in formation of anomalous waves of the limiting steepness.

moment of maximal amplitude, at $M = 0$ and $C = 0$ can be found from the simple condition $\sinh 2\xi_1 = 1/N$, as it is clear in view of formula (24).

It is worth noting that at $M = 0$ the cyclic variable χ remains constant, as it follows from Eq.(10). As we shall see soon, the physical wave fields corresponding to different values of χ , strongly differ between each other. In particular, at $\chi = 0$ the wave picture is symmetric with respect to sign change of y coordinate, while at $\chi \neq 0$ there is no any symmetry (see Figs.2-3). But in the framework of NLSE, the envelope of one solution coincides with the envelope of the other solution after a hyperbolic rotation of the dimensionless coordinates. The presence of this approximate symmetry significantly clarifies the question about optimal conditions for the formation of anomalous waves.

V. COMPARISON WITH NUMERICAL EXPERIMENTS

It is clear that any simplified model without verification remains just a toy. In order to make the status of the variational approximation more distinct, it is necessary to compare it with a more accurate model. In our case, numerical experiments were carried out in the framework of the fully nonlinear long-crested wave model which is described in detail in Refs.[38, 39]. The computational domain was a square of the size 5 km, with the periodic

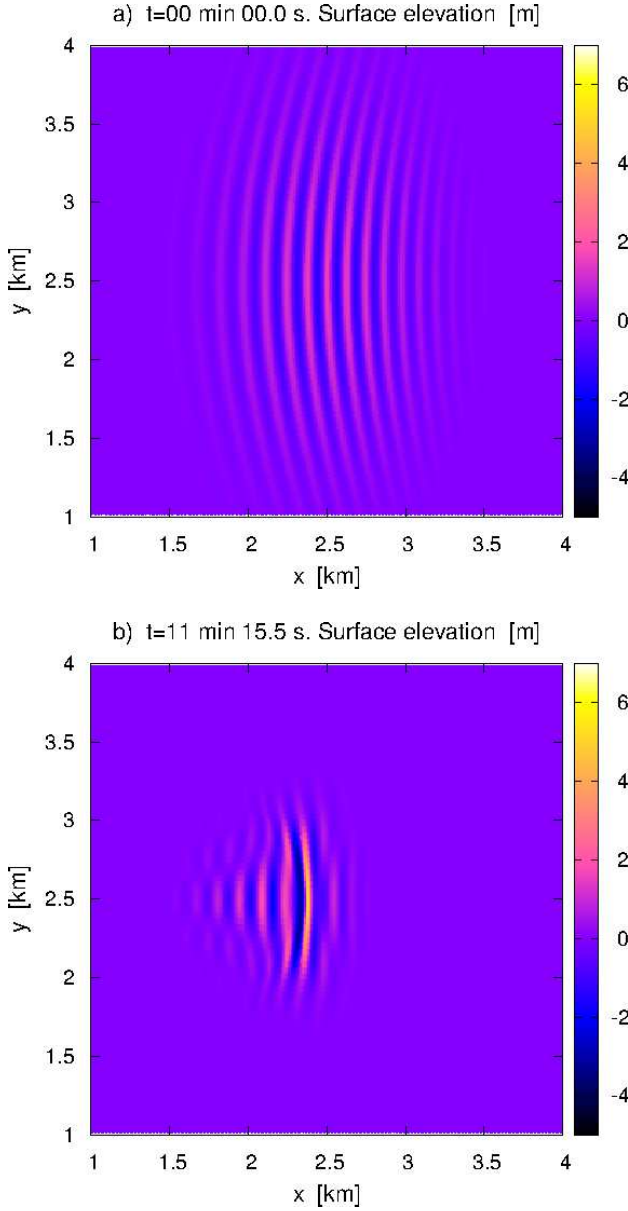


FIG. 2: Wave picture at $\chi = 0.0$ (the other parameters are the same as in Fig.1): a) wave packet at the initial time moment; b) at the moment when the anomalous wave has risen. The crest length of the high wave here has been much longer than it would be in the linear case, which observation is in accordance with the Gaussian model prediction. Deviations from the Gaussianity are clearly seen, basically — in the form of a small tail consisting of longer waves.

boundary conditions. The length of the carrier wave was chosen $\lambda_0 = 125$ m. The simulations were carried out for different sets of initial parameters of the packet.

In Fig.2a and Fig.3a, examples are shown of how Gaussian initial conditions look. The “portraits” of anomalous waves developing from those conditions, are presented in Fig.2b and Fig.3b. In general, deviations from the Gaussian shape are clearly seen there. Despite the non-

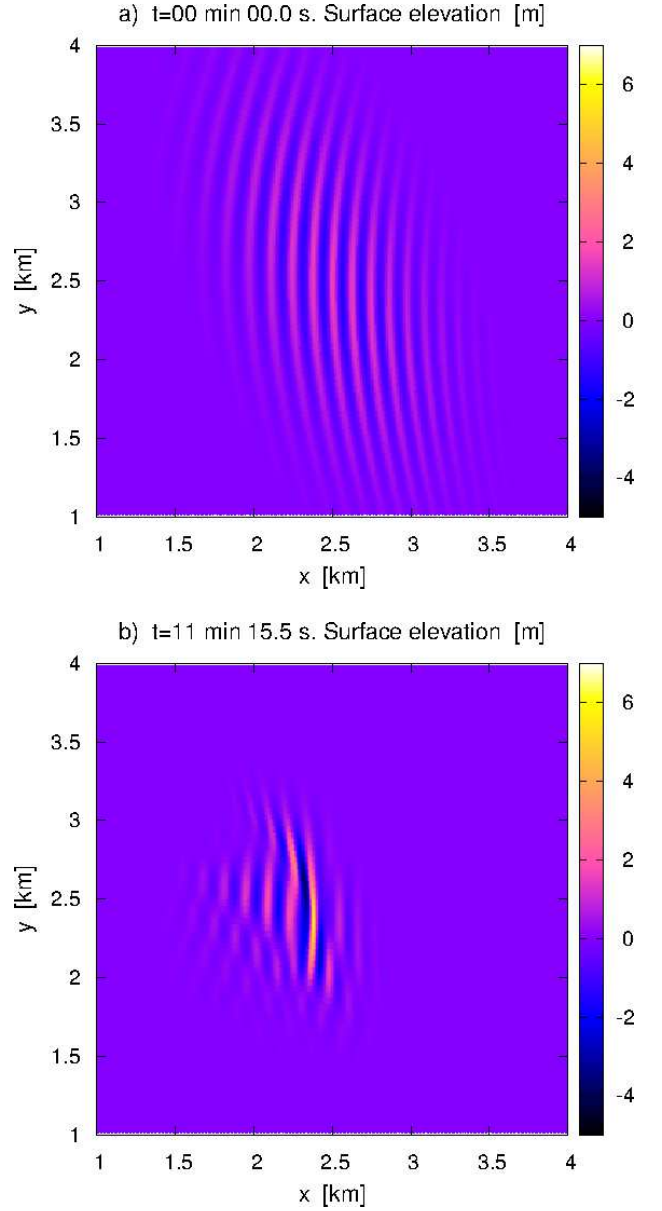


FIG. 3: Wave picture at $\chi = 0.3$ (the other parameters are the same as in Fig.1): a) wave packet at the initial time moment; b) at the moment of the anomalous wave rise. Deviations from the Gaussianity are even more prominent here than at $\chi = 0.0$.

Gaussianity of the arising rogue waves, Figs.4-5 demonstrate that there is a qualitative agreement between the variational theory and the numerical experiment in the important aspect as the temporal dependence of the maximal amplitude of the wave packet. It is seen that Gaussian model somewhat overestimates the height of anomalous wave (especially as parameter χ increases to values about unity, when the approximate symmetry of the hyperbolic rotation becomes invalid), and it moves to the future the moment of the maximal rise. However, it is

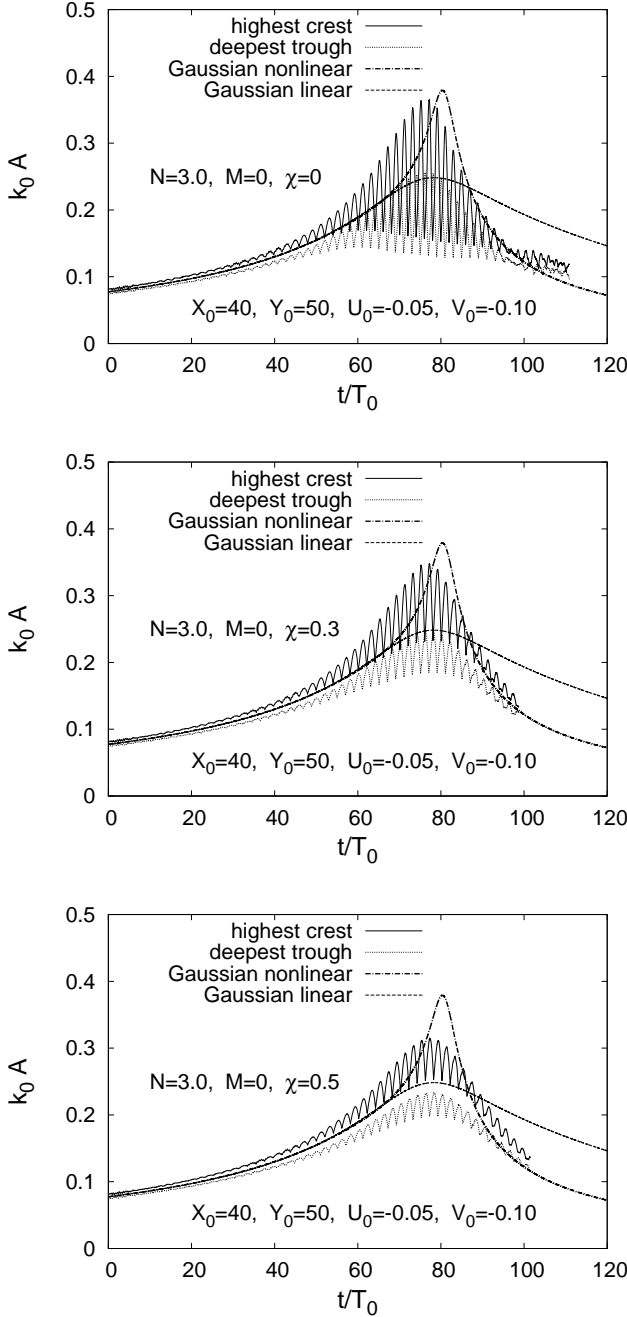


FIG. 4: Comparison of the temporal dependencies of the maximal amplitudes for wave packets with different χ , the other parameters being the same as in Fig.1. In each figure shown are numerically found the height of the highest crest and the depth of the deepest trough, and also predictions of the Gaussian models — linear and nonlinear. The numerical curves have an oscillating character, which property is related to the approximately two-fold difference between the phase velocity of the carrier wave and the group velocity of the packet motion. Heights of crests are typically larger than depths of troughs, due to the presence of higher harmonics. Therefore the quantity that should be compared to the theoretical predictions is a half-sum of envelopes of the numerical curves.

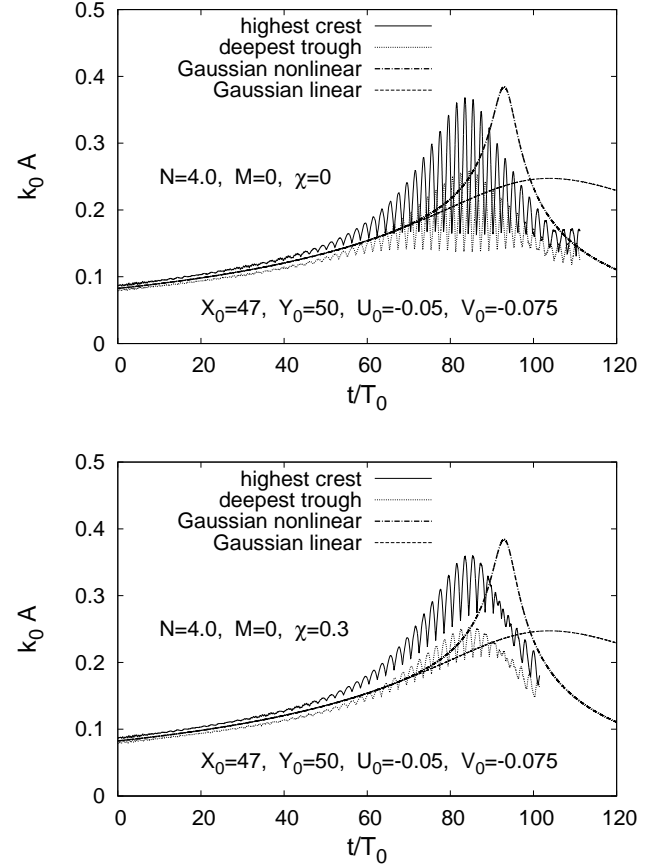


FIG. 5: Comparison of the maximal amplitudes for different sets of initial data than in Fig.4. It is seen that with increase of N , the time delay of the predicted peak in comparison with the numerical simulation increases.

hardly reasonable to expect a detailed accordance from the simplest variational approximation. In any case, the time period of existence of anomalous wave is predicted by the Gaussian theory rather well. Also another important effect is confirmed, the increase of the transverse packet size as compared to the linear theory (see Fig.1). This effect contributes to the subsequent more fast decrease of the amplitude in comparison with the linear case.

VI. CONCLUSIONS

Thus, based on the variational analysis and on the comparison with the results of direct numerical simulations, it is natural to put forward the following thesis. In the main approximation, a typical long-crested three-dimensional oceanic rogue wave at the nonlinear stage is, from the mathematical point of view, a dynamical system with just two degrees of freedom: $X(t)$ and $Y(t)$. This system contains two constant parameters (N

and M), which are related to the integrals of motion of 1+2D NLSE and characterize a given group of waves. The system is integrable. Real sea states where one can expect anomalous waves, require values $N \approx 2-4$. The most favorable focusing parameters for the rogue wave formation are: 1) $M \approx 0$; 2) on the initial stage of (oc-

casional) focusing at some time moment t_* the relations $X_* \approx Y_* \sim 20-40$, $-\dot{X}_* \approx -\dot{Y}_* \gtrsim 0.05$ should take place. To estimate probability of realization of such conditions in random weakly nonlinear wave fields is the task on the future.

-
- [1] C. Kharif and E. Pelinovsky, Eur. J. Mech. B/Fluids **22**, 603 (2003).
 - [2] K. Dysthe, H. E. Krogstad, and P. Müller, Annu. Rev. Fluid Mech. **40**, 287 (2008).
 - [3] M. Onorato, S. Residori, U. Bortolozzo, A. Montina, and F. T. Arecchi, Physics Reports **528**, 47 (2013).
 - [4] V. E. Zakharov, J. Appl. Mech. Tech. Phys. **9**, 190 (1968).
 - [5] T. B. Benjamin and J. E. Feir, J. Fluid Mech. **27**, 417 (1967).
 - [6] V. E. Zakharov, A. I. Dyachenko, and O. A. Vasilyev, Eur. J. Mech. B/Fluids **21**, 283 (2002).
 - [7] A. I. Dyachenko and V. E. Zakharov, JETP Letters **81**, 255 (2005).
 - [8] V. E. Zakharov, A. I. Dyachenko, and O. A. Prokofiev, Eur. J. Mech. B/Fluids **25**, 677 (2006).
 - [9] V. P. Ruban, JETP Letters **95**, 486 (2012).
 - [10] A. Chabchoub, N. P. Hoffmann, and N. Akhmediev Phys. Rev. Lett. **106**, 204502 (2011).
 - [11] A. Chabchoub, N. Hoffmann, M. Onorato, and N. Akhmediev, Phys. Rev. X **2**, 011015 (2012).
 - [12] N. Akhmediev, V. M. Eleonskii, and N. E. Kulagin, Sov. Phys. JETP **62**, 894 (1985).
 - [13] N. Akhmediev and V. Korneev, Theor. Math. Phys. **69**, 1089 (1986).
 - [14] N. N. Akhmediev, V. M. Eleonskii, and N. E. Kulagin, Theor. Math. Phys. **72**, 809 (1987).
 - [15] N. Akhmediev, A. Ankiewicz, and J. M. Soto-Crespo Phys. Rev. E **80**, 026601 (2009).
 - [16] M. Erkintalo, K. Hammami, B. Kibler, C. Finot *et al.*, Phys. Rev. Lett. **107**, 253901 (2011).
 - [17] M. Onorato, A. R. Osborne, and M. Serio, Phys. Rev. Lett. **96**, 014503 (2006).
 - [18] M. Onorato, T. Waseda, A. Toffoli, L. Cavaleri *et al.*, Phys. Rev. Lett. **102**, 114502 (2009).
 - [19] V. P. Ruban, Phys. Rev. E **74**, 036305 (2006).
 - [20] V. P. Ruban, Phys. Rev. Lett. **99**, 044502 (2007).
 - [21] D. H. Peregrine, Adv. Appl. Mech. **16**, 9 (1976).
 - [22] I. V. Lavrenov and A. V. Porubov, Eur. J. Mech. B/Fluids **25**, 574 (2006).
 - [23] V. I. Shrira and A. V. Slunyaev, Phys. Rev. E **89**, 041002(R) (2014).
 - [24] C. Fochesato, S. Grilli, and F. Dias, Wave Motion **44**, 395 (2007).
 - [25] V. P. Ruban, JETP Letters **97**, 686 (2013).
 - [26] M. Desaix, D. Anderson, and M. Lisak, J. Opt. Soc. Am. B **8**, 2082 (1991).
 - [27] L. Bergé, Phys. Lett. A **189**, 290 (1994).
 - [28] L. Bergé and J. J. Rasmussen, Phys. Rev. E **53**, 4476 (1996).
 - [29] L. Bergé, J. J. Rasmussen, E. A. Kuznetsov, E. G. Shapiro, and S. K. Turitsyn, J. Opt. Soc. Am. B **13**, 1879 (1996).
 - [30] L. Berge, Phys. Reports **303**, 259 (1998).
 - [31] V. M. Pérez-García, H. Michinel, J. I. Cirac, M. Lewenstein, and P. Zoller, Phys. Rev. Lett. **77**, 5320 (1996); Phys. Rev. A **56**, 1424 (1997).
 - [32] Yu. Kagan, E. L. Surkov, and G. V. Shlyapnikov, Phys. Rev. A **55**, R18 (1997).
 - [33] Y. Castin and R. Dum, Phys. Rev. Lett. **77**, 5315 (1996).
 - [34] F. Haas, Phys. Rev. A **65**, 033603 (2002).
 - [35] A. S. Desyatnikov, D. Buccoliero, M. R. Dennis, and Yu. S. Kivshar, Phys. Rev. Lett. **104**, 053902 (2010).
 - [36] J. Abdullaev, A. S. Desyatnikov, and E. A. Ostrovskaya, J. Opt. **13**, 064023 (2011).
 - [37] V. P. Ruban, JETP Letters **100**, 751 (2014).
 - [38] V. P. Ruban and J. Dreher, Phys. Rev. E **72**, 066303 (2005).
 - [39] V. P. Ruban, Eur. Phys. J. Special Topics **185**, 17 (2010).